CLINICAL AND VACCINE IMMUNOLOGY, Jan. 2007, p. 74–80 Vol. 14, No. 1
1556-6811/07/$08.00+0 doi:10.1128/CVI.00250-06

CD27 and CD57 Expression Reveals Atypical Differentiation of Human Immunodeficiency Virus Type 1-Specific Memory CD8$^+$ T Cells$^\nabla$

Aki Hoji,[1]† Nancy C. Connolly,[2] William G. Buchanan,[1] and Charles R. Rinaldo, Jr.[1,3]*

Department of Infectious Diseases and Microbiology, Graduate School of Public Health,[1] and Departments of Medicine[2] and Pathology,[3] School of Medicine, University of Pittsburgh, Pittsburgh, Pennsylvania 15261

Received 8 July 2006/Returned for modification 16 August 2006/Accepted 23 October 2006

The failure of human immunodeficiency virus type 1 (HIV-1)-specific CD8$^+$ T cells to control chronic HIV-1 infection could be due to the progressive loss of their capacities to undergo normal memory effector differentiation. We characterized and compared the expressions of CD27, CD28, CD57, and CD62L by Epstein-Barr virus (EBV)-, cytomegalovirus (CMV)-, and HIV-1-specific CD8$^+$ T cells by six-color, eight-parameter flow cytometry. In contrast to the maturation of EBV- and CMV-specific memory CD8$^+$ T cells, we found that HIV-1-specific CD8$^+$ T cells did not display coordinated down-regulation of CD27 and up-regulation of CD57 and accumulated in an atypical CD27^{high} CD57^{low} subset. Moreover, the accumulation of CD27^{high} CD57^{low} HIV-1-specific CD8$^+$ T cells was positively correlated with HIV-1 plasma viremia. The differentiation of HIV-1-specific CD8$^+$ T cells to an effector subset is therefore impaired during chronic HIV-1 infection. This lack of normal CD8$^+$ T-cell differentiation could contribute to the failure of cellular immune control of HIV-1 infection.

Understanding CD8$^+$ T-cell memory effector differentiation is essential for studying how virus-specific CD8$^+$ T cells control viral infection. Distinct stages of virus-specific CD8$^+$ T-cell memory effector differentiation have been extensively characterized by phenotypic and functional analyses. Primed virus-specific CD8$^+$ T cells typically differentiate from the least mature memory stage (CD27$^+$ CD28$^+$ CD45RO$^+$) to the most mature effector stage (CD27$^-$ CD28$^-$ CD45RA$^+$) (3, 13). Terminally differentiated effector cells can be further defined by CD57 expression (4).

The association of phenotypes of human immunodeficiency virus type 1 (HIV-1)-specific CD8$^+$ T cells with disease progression remains controversial. While HIV-1-specific CD8$^+$ T cells in long-term nonprogressors have been reported to be phenotypically enriched for an effector subset (CD27$^-$ CD45RA$^+$) (12), others have reported that HIV-1-specific CD8$^+$ T cells remain enriched in an intermediate stage (CD27$^+$ CD28$^-$) regardless of clinical status (9) and duration of infection (2). It is not clear from these latter studies, however, whether the differentiation of HIV-1-specific CD8$^+$ T cells during chronic HIV-1 infection is impaired prior to the effector stage. Moreover, since continuous replication of HIV-1 during chronic persistent infection provides a constant supply of HIV-1 antigens, long-term HIV-1 infection should theoretically drive HIV-1-specific CD8$^+$ T cells to the effector stage. Phenotypic enrichment observed in these studies (2, 9), therefore, could be a consequence of a blockade in CD8$^+$ T-cell differentiation prior to the effector stage. Thus, HIV-1-specific CD8$^+$ T-cell memory effector differentiation needs to be clarified in relation to the natural course of memory CD8$^+$ T-cell differentiation.

In the present study, we assessed the differentiation of HIV-1-specific CD8$^+$ T cells by phenotypic analysis based on CD27, CD28, CD57, and CD62L expression in a cohort of HIV-1-infected subjects with a range of T-cell counts and viral loads and uninfected participants. We found that, in contrast to Epstein-Barr virus (EBV)- and cytomegalovirus (CMV)-specific CD8$^+$ T cells, the majority of HIV-1-specific CD8$^+$ T cells were phenotypically enriched in CD27^{high} CD57$^-$ and CD27^{high} CD57^{low} subsets and showed no evidence of progression to the effector subset (CD27$^-$ CD57^{high}). These results suggest that the phenotypic enrichment of HIV-1-specific CD8$^+$ T cells that persists in spite of the continuous presence of HIV-1 antigen is due to impaired CD8$^+$ T-cell effector differentiation.

(This work was in partial fulfillment of the requirements for a Ph.D. for A.H. from the University of Pittsburgh.)

MATERIALS AND METHODS

Study population. The study population consisted of 11 HIV-1-uninfected participants (median age, 52 years; range, 43 to 69 years; 1 female and 10 male Caucasians) and 7 HIV-1-infected participants (median age, 48 years; range, 25 to 70 years; all male Caucasians) from the Pittsburgh portion of the Multicenter AIDS Cohort Study with a range of HLA types, CD4$^+$ T-cell counts (median, 453; range, 129 to 1,029 cells/mm^3), and viral loads (median, 22,580; range, 101 to 66,750) (Table 1). None of the HIV-1-infected subjects were on antiretroviral therapy at the time of this study. The HIV-1 plasma viral load was measured by a quantitative reverse transcription-PCR assay (Amplicor; Roche Diagnostics, Alameda, CA). HLA typing was performed at the Laboratory of Genomic Diversity, National Cancer Institute, and the laboratory of M. Trucco, University of Pittsburgh.

* Corresponding author. Mailing address: A419 Crabtree Hall, Graduate School of Public Health, University of Pittsburgh, Pittsburgh, PA 15261. Phone: (412) 624-3928. Fax: (412) 624-4953. E-mail: rinaldo@pitt.edu.

† Present address: Department of Medicine, Division of Infectious Diseases, University of California-Los Angeles, Los Angeles, CA 90095.

$^\nabla$ Published ahead of print on 1 November 2006.

TABLE 1. HLA types, tetramer reactivity, and clinical data of study participants

Identification no.	HLA type	Tetramer reactivity[a]	Clinical status[b]	CD4 count[c]	Viral load[d]
1	A1, A3, B8, B53	B8p24, B8nef	HIV-1+	270	18,646
2	A2, A3, B57, B40	A2p17, A2pol, A3p17, A2EBV, A2CMV	HIV-1+	129	66,752
3	A2, A3, B27, B37	A2p17, A2pol, A2EBV, A2CMV	HIV-1+	459	939
4	A2, A33, B15, B42	A2p17	HIV-1+	1,029	101
5	A2, B27, B13	A2p17, A2pol, A2EBV, A2CMV	HIV-1+	990	23,737
6	A3, A31, B13, B51	A3p17, A3pol	HIV-1+	453	22,580
7	A3, A24, B27, B15	A3p17, A3pol	HIV-1+	385	24,968
8	A2	A2CMV	HIV-1−		
9	A2, B8	A2EBV, B8EBV	HIV-1−		
10	A2, A31, B15, B44	A2CMV	HIV-1−		
11	A2, A24, B44, B7	A2EBV, A2CMV	HIV-1−		
12	A2	A2CMV	HIV-1−		
13	A1, A2, B8, B56	A2CMV	HIV-1−		
14	A1, A11, B8, B15	B8EBV	HIV-1−		
15	A1, A2, B18, B51	A2EBV, A2CMV	HIV-1−		
16	A2, A23, B13, B44	A2CMV	HIV-1−		
17	A2, A23, A39, B41	A2CMV	HIV-1−		
18	A2, A24, A44, A15	A2CMV	HIV-1−		

[a] Each tetramer is designated by the HLA type and the antigen.
[b] Clinical status of study participants at the time of their blood draw. HIV-1+ and HIV-1− indicate HIV-1-infected and uninfected individuals, respectively.
[c] CD4 count indicates a number of CD4+ T cells per milliliter of blood.
[d] Viral load indicates a number of HIV-1 viral genomes per milliliter of a serum sample.

Antibodies and major histocompatibility complex class I (MHC-I) tetramers. The following monoclonal antibodies (MAbs) were used: fluorescein isothiocyanate-conjugated mouse anti-human CD57 and phycoerythrin (PE)-Cy5-conjugated mouse anti-human CD27 (BD Biosciences, San Jose, CA); ECD (PE–Texas Red)-conjugated mouse anti-human CD28 and PE-Cy7-conjugated mouse anti-human CD8 (Coulter-Immunotech, Miami, FL); and allophycocyanin-Cy7-conjugated mouse anti-human CD62L (Caltag, Burlingame, CA). Appropriate isotype-matched MAbs were obtained from the same companies and used throughout the course of the study.

MHC-I tetrameric reagents used in the study are listed in Table 2. All of the tetrameric agents except A2pp65 CMV and A2BMLF1 EBV were obtained from the NIH Tetramer Synthesis Facility. A2pp65 CMV and A2BMLF1 EBV tetramers were obtained from Coulter Immunomics (San Diego, CA). All of the tetramers were labeled with PE and used at a 1/50 to 1/200 dilution for staining 2×10^6 to 5×10^6 peripheral blood mononuclear cells (PBMCs).

Isolation and preparation of stained PBMCs. Blood specimens were collected in BD Vacutainer cell preparation tubes with sodium heparin (BD Biosciences, San Jose, CA), and PBMCs were isolated according to the manufacturer's protocol. PBMCs were stained as described previously (8), with modifications. Briefly, 2×10^6 to 5×10^6 fresh PBMCs were resuspended in RPMI 1640 medium (GIBCO, Grand Island, NY) with 10% heat-inactivated fetal calf serum (HyClone, Logan, UT) and stained with a 1/50 to 1/200 dilution of the appropriate tetramer at 37°C for 25 min. The cells were then washed and resuspended in phosphate-buffered saline with 4% fetal calf serum and 0.1% sodium azide and incubated with a cocktail of MAbs for 30 min at 4°C. After the final wash, cells were fixed with 1% paraformaldehyde and analyzed with a MoFlo flow cytometer (DakoCytomation, Boulder, CO).

TABLE 2. List of epitopes used for MHC class I tetramer analysis

HLA allele	Epitope amino acid sequence	Protein	Epitope location[a]
A2	SLYNTVATL	HIV-1 p17Gag	77–85
A2	ILKEPVHGV	HIV-1 Pol	309–317
A2	GLCTLVAML	EBV BMLF1	280–288
A2	NLVPMVATV	CMV pp65	495–503
A3	RLRPGGKKK	HIV-1 p17Gag	20–28
A3	AIFQSSMTK	HIV-1 Pol	158–166
A3	QVPLRPMTYK	HIV-1 Nef	73–82
B8	EIYKRWII	HIV-1 p24Gag	128–135
B8	FLKEKGGL	HIV-1 Nef	90–97
B8	RAKFKQLL	EBV BZLF1	190–197

[a] Epitope location is indicated by number of amino acids spanning the epitope from N terminus of the corresponding protein.

Flow cytometry. The MoFlo flow cytometer was calibrated for laser fluctuation/alignment and photomultiplier tube voltage adjustment by using FlowCheck beads (Coulter, Miami, FL) and Ultra Rainbow Calibration beads (Spherotech, Inc., Libertyville, IL) prior to the sample acquisition. A six-color compensation matrix was created by FlowJo (TreeStar, Cupertino, CA), which was based on six singly stained PBMC samples from actual donors. A PE-conjugated mouse anti-human CD8 MAb was used for PE compensation in place of the MHC-I tetramer.

We used a flow cytometric analysis described previously (8) with a few modifications. A minimum of 500 total tetrameter-positive $CD8^{high}$ events were collected for the fully stained sample and isotype control (the same number of events were collected for both samples), and this resulted in a collection of approximately 1×10^6 to 3×10^6 total events. We used a compounded gating scheme as previously described (7, 8), with necessary modifications. Briefly, cells were first gated on the $CD8^{high}$ population on a CD8 and side scatter (SS)-log plot, followed by a lymphocyte gate on an forward scatter (FS)- and SS-log plot. Potential doublets were excluded based on an FS-area and FS-height plot. The resulting tetrameter-positive population was visualized on a tetramer-PE versus SS-log plot for determining phenotypic analysis and the frequency of tetrameter-positive CD8+ T cells. Proper gating was established by using tetramer and CD8-PECy7 doubly stained cells in the presence of fluorescent-labeled isotype controls. Data analysis and graphic representations were performed with FlowJo software.

Statistical analysis. We used analysis of variance and the Tukey-Kramer honest significant difference test for determining statistical significance between and among group means. We used the two-tailed Spearman correlation test for determining P values and a standard least square method for determining R^2 correlation coefficients. A P value of <0.05 was considered statistically significant. Statistical analysis and graphical representation were performed using JMP IN, version 5.1 (JMP Sales, Cary, NC), and Aabel software (Gigawiz Ltd. Co., Tulsa, OK).

RESULTS

EBV-, CMV-, and HIV-1-specific CD8+ T cells show distinct levels of CD27, CD28, CD57, and CD62L expression. We first used a battery of phenotypic markers and MHC-I tetramers to assess virus-specific T-cell phenotypes comparable to those previously related to a unique virus-specific memory CD8+ T cell during persistent viral infections (1). Virus-specific CD8+

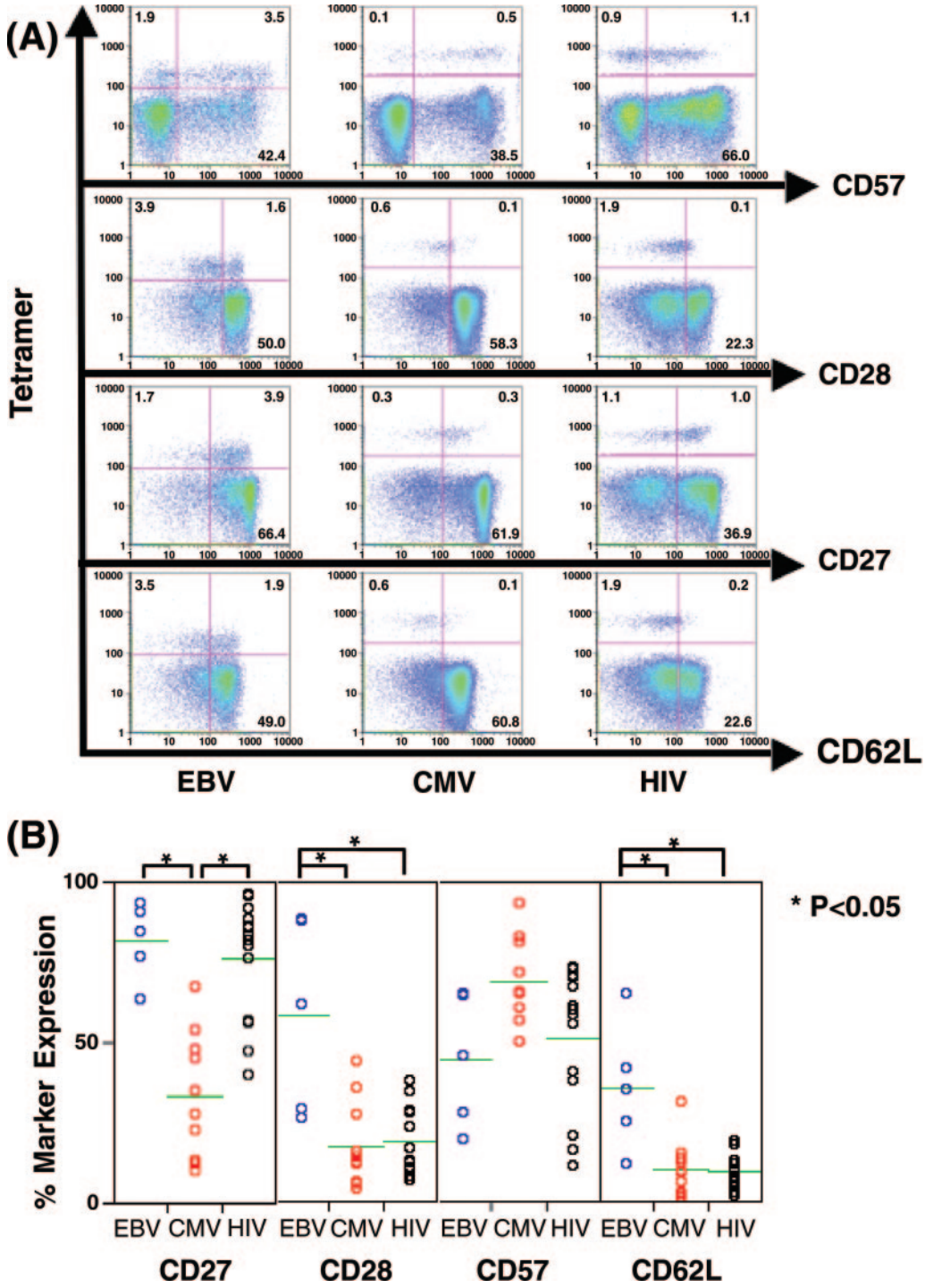

FIG. 1. Visualization of virus-specific $CD8^+$ T cells by staining ex vivo with MHC-I tetramers and surface expression of memory/effector phenotypic markers. All cells shown are a result of compound gating; an initial gate was set on the $CD8^{high}$ subset on CD8 and SS-log, followed by a lymph-gate on FS-area and SS-log. (A) Representative figure showing surface expression of CD27, CD28, CD57, and CD62L on EBV-, CMV-, and HIV-1-specific $CD8^+$ T cells. Numbers in the quadrants indicate percentages of cells. (B) Comparison of percentages of CD27, CD28, CD57, and CD62L expressing EBV-, CMV-, and HIV-1-specific $CD8^+$ T cells. Data are from the participants with EBV tetramer reactivity ($n = 5$), CMV tetramer reactivity ($n = 9$), and HIV-1 tetramer reactivity ($n = 14$).

T cells were visualized by a host of MHC-I tetramers, and the phenotypes of virus-specific $CD8^+$ T cells were assessed by costaining with antibodies against CD27, CD28, CD57, and CD62L (Fig. 1A).

Comparison of percent surface marker expression revealed phenotypic subsets unique to each type of virus-specific $CD8^+$ T cell (Fig. 1B). The proportion of the $CD27^+$ CMV-specific $CD8^+$ T cell (median 31%; range 10 to 67%) significantly

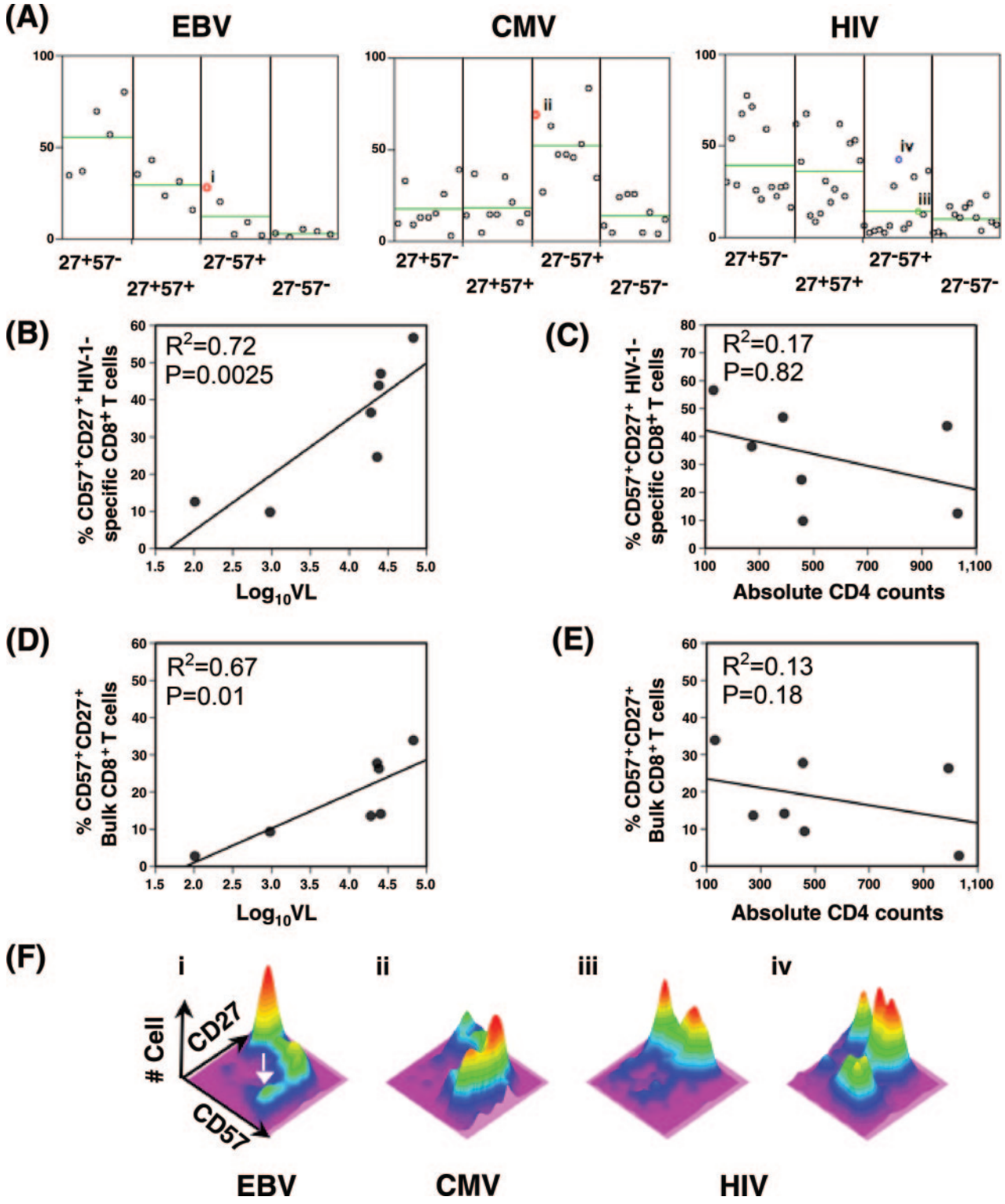

FIG. 2. HIV-1-specific $CD8^+$ T cells do not show effector maturation-associated progression from the $CD27^{high}$ $CD57^-$ subset to the $CD27^-$ $CD57^{high}$ subset. (A) Proportions of four binary CD27 CD57 subsets of EBV-, CMV-, and HIV-1-specific $CD8^+$ T cells are compared. The green line indicates the mean of each subset. Data are from the participants with EBV tetramer reactivity ($n = 5$), CMV tetramer reactivity ($n = 9$), and HIV-1 tetramer reactivity ($n = 14$). (B to E) Proportions of the $CD27^+$ $CD57^+$ ($CD27^{high}$ $CD57^{low}$) subsets of HIV-1-specific and bulk $CD8^+$ T cells positively correlated with HIV-1 plasma viral load (B and D) but not with absolute CD4 counts (C and E). HIV-specific $CD8^+$ T cells from HIV-infected individuals ($n = 7$) are plotted against HIV-1 plasma viral load ($\log_{10}$VL). Mean values of corresponding percent $CD27^+$ $CD57^+$ of HIV-specific and bulk $CD8^+$ T cells are used for those with multiple HIV-1-specific tetramer reactivity. (F) Representative three-dimensional topographical plots of CD27 and CD57 expression on EBV (panel i)-, CMV (panel ii)-, and HIV-1 (panels iii and iv)-specific $CD8^+$ T cells are shown. Color variation indicates a number of cells from low (purple) to high (red) on a z axis. The white arrow indicates the $CD27^-$ $CD57^{high}$ subset. Percent $CD27^-$ $CD57^+$ of representative results (colored circles) are shown in Fig. 2A. Panels i and ii represent EBV- and CMV-specific $CD8^+$ T cells from HIV-1 uninfected (red circles, participants 9 and 8, respectively), while panels iii (green circle, B8nef from participant 1), and iv (blue circle, A3pol from participant 7) represent HIV-1-infected participants.

differed from the proportions of the $CD27^+$ HIV-1-specific (median, 83%; range, 40 to 96%) and the $CD27^+$ EBV-specific $CD8^+$ T cells (median, 85%; range, 63 to 93%) ($P < 0.05$). There were also significant differences in the proportion of $CD28^+$ and $CD62L^+$ subsets between HIV-1-specific (for CD28, median, 15%, and range, 6 to 38%; for CD62L, median, 9%, and range, 2 to 19%) or CMV-specific (for CD28, median, 13%, and range, 4 to 44%; for CD62L, median, 9%, and range, 1 to 31%) $CD8^+$ T cells, and EBV-specific $CD8^+$ T cells (for CD28, median, 61%, and range, 26 to 88%; for CD62L, median, 35%, and range, 12 to 65%) ($P < 0.05$). There were no significant differences in the proportions of the $CD57^+$ subset, although the percentages of $CD8^+$ $CD57^+$ T cells specific for CMV-specific $CD8^+$ T cells were slightly higher than the $CD57^+$ EBV- or HIV-1-specific $CD8^+$ T cells. Based on these results, the major phenotypic subsets of EBV-, HIV-1-, and CMV-specific $CD8^+$ T cells appeared to be $CD27^+$ $CD28^+$ $CD57^-$ $CD62L^{+/-}$, $CD27^+$ $CD28^-$, $CD57^+CD62L^-$ and $CD27^-$ $CD28^-$ $CD57^+$ $CD62L^-$, respectively. Thus, HIV-1-specific $CD8^+$ T cells from a cohort of HIV-1-infected participants were phenotypically in an intermediate stage of $CD8^+$ T-cell differentiation. This is in agreement with observations made by Appay et al. (1).

Correlation between proportions of $CD27^+$ $CD57^+$ HIV-1-specific $CD8^+$ T cells and plasma viral load. We assessed CD57 expression as a surrogate marker of terminal differentiation. The majority of HIV-1-specific $CD8^+$ T cells were enriched evenly ($P > 0.05$) in $CD27^+$ $CD57^-$ (median, 28%; range, 16 to 77%) and $CD27^+$ $CD57^+$ (median, 36%; range, 8 to 67%) subsets (Fig. 2A). In contrast, CMV-specific $CD8^+$ T cells were enriched predominantly in the $CD27^-$ $CD57^+$ (median, 47%; range, 17 to 84%) subset ($P < 0.05$), and EBV-specific $CD8^+$ T cells were relatively more enriched in the $CD27^+$ $CD57^-$ (median, 56%; range, 35 to 80%) subset.

We found that the percentage of $CD27^+$ $CD57^+$ HIV-1-specific $CD8^+$ T cells strongly correlated with the plasma viral load ($R^2 = 0.72$; $P = 0.0025$) (Fig. 2B), while proportions of $CD27^+$ $CD57^-$ ($R^2 = 0.66$; $P = 0.18$), $CD27^-$ $CD57^+$ ($R^2 = 0.15$; $P = 0.88$), and $CD27^-$ $CD57^-$ other subsets ($R^2 = 0.09$; $P = 0.11$) did not (data not shown). Moreover, bulk $CD8^+$ T cells from the same HIV-1-infected participants showed a positive correlation (Fig. 2D) ($R^2 = 0.67$; $P = 0.01$), suggesting that progression to the $CD27^{high}$ $CD57^{low}$ subset is not strictly limited to HIV-1-specific $CD8^+$ T cells, whereas other subsets, $CD27^+$ $CD57^-$ ($R^2 = 0.66$; $P = 0.21$), $CD27^-$ $CD57^+$ ($R^2 = 0.15$; $P = 0.45$), and $CD27^-$ $CD57^-$ subsets ($R^2 = 0.09$; $P = 1.00$), did not (data not shown). This suggests that progression to the $CD27^{high}$ $CD57^{low}$ subset is not strictly limited to HIV-1-specific $CD8^+$ T cells. There was no correlation between absolute $CD4^+$ T-cell counts and the proportion of $CD27^+$ $CD57^+$ HIV-1-specific $CD8^+$ T cells or the bulk $CD27^+$ $CD57^+$ $CD8^+$ T cell (Fig. 2C and E, respectively) or other T-cell subsets (data not shown).

Progression of the HIV-1-specific $CD8^+$ T cell to the atypical $CD27^{high}$ $CD57^{low}$ subset. Notably, the pattern of CD27 and CD57 expression revealed an additional aspect of virus-specific memory $CD8^+$ T-cell differentiation. EBV- and CMV-specific $CD8^+$ T cells appeared to uninterruptedly progress from $CD27^{high}$ $CD57^-$ (undifferentiated memory stage) to $CD27^-$ $CD57^{high}$ (effector stage) (Fig. 2F). This pattern of progression from an immature to mature stage was apparent in the relatively more differentiated EBV-specific $CD8^+$ T cells (Fig. 2F, panel i) and in most of the CMV-specific $CD8^+$ T cells (Fig. 2F, panel ii). In contrast, the $CD57^+$ subset of HIV-1-specific $CD8^+$ T cells typically appeared in the absence of CD27 down-regulation (Fig. 2F, panel iii). This pattern persisted even in HIV-1-specific $CD8^+$ T cells with the highest proportion of the $CD27^-$ $CD57^+$ subset (Fig. 2F, panel iv). Also, virtually all the $CD27^+$ $CD57^+$ HIV-1-specific $CD8^+$ T cells were $CD27^{high}$ $CD57^{low}$ (Fig. 3).

Three HIV-1-infected participants (Table 1) had EBV- and/or CMV-specific $CD8^+$ T cells, making it possible to compare the phenotypes of these virus-specific $CD8^+$ T cells from the same immunological background. EBV-specific $CD8^+$ T cells from these HIV-1-infected participants appeared to be phenotypically enriched in the immature stage ($CD27^{high}$ $CD57^-$), similar to the same cells from HIV-1-uninfected participants. Similarly, CMV-specific $CD8^+$ T cells did not appear to accumulate the atypical $CD27^{high}$ $CD57^{low}$ phenotype and showed the expected pattern of CD27 and CD57 expression (Fig. 3). In contrast, $CD8^+$ T cells specific for the HIV-1 p17 epitope (SLYNVATL) from two participants with high viral load (Table 1) accumulated in the atypical $CD27^{high}$ $CD57^{low}$ subset (Fig. 3B and C), whereas the same cell from a participant with a relatively lower viral load and higher CD4 counts rarely accumulated in the atypical $CD27^{high}$ $CD57^{low}$ subset (Fig. 3A). Interestingly, $CD8^+$ T cells specific for HIV-1 polymerase epitope (ILKEPVHGV) did not show a similar level of $CD27^{high}$ $CD57^{low}$ accumulation. In fact, there was no statistically significant difference in the proportion of the $CD27^{+(high)}$ $CD57^{+(low)}$ subset between $CD8^+$ T cells specific for HIV Gag and HIV Pol epitopes ($P > 0.05$) (data not shown). However, the development of the atypical $CD27^{high}$ $CD57^{low}$ subset from the $CD27^{high}$ $CD57^-$ subset (undifferentiated) was clearly demonstrated (Fig. 3B and 3C).

Based on these results, HIV-1-specific $CD8^+$ T cells appear to differentiate to an atypical subset ($CD27^{high}$ $CD57^{low}$) rather than to the typical effector subset ($CD27^-$ $CD57^{high}$), even in the continuous presence of HIV-1 antigens. Furthermore, progression to the $CD27^{high}$ $CD57^{low}$ subset is positively correlated with HIV-1 viremia but not with absolute $CD4^+$ T-cell counts.

DISCUSSION

We show that the majority of HIV-1-specific $CD8^+$ T cells in participants with chronic, untreated HIV-1 infection displayed the phenotype $CD27^+$ $CD28^-$ $CD57^{-/low}$ $CD62L^-$, suggestive of the advanced intermediate stage of $CD8^+$ T-cell differentiation. Previous studies have shown that HIV-1-specific $CD8^+$ T cells lack CD62L expression (5) and are phenotypically enriched in the intermediate stage of $CD8^+$ T-cell differentiation (1, 2, 9, 12). More recent studies have found a correlation between an increasing proportion of $CD57^+$ HIV-specific $CD8^+$ T cells and disease progression (4, 10).

A novel finding of our study is the development and accumulation of the previously uncharacterized $CD27^{high}$ $CD57^{low}$ subset of HIV-1-specific $CD8^+$ T cells, which is significantly correlated with plasma viral load. Since the functional significance of the $CD27^{high}$ $CD57^{low}$ subset is unknown at present, it is difficult to address the cause-and-effect relationships be-

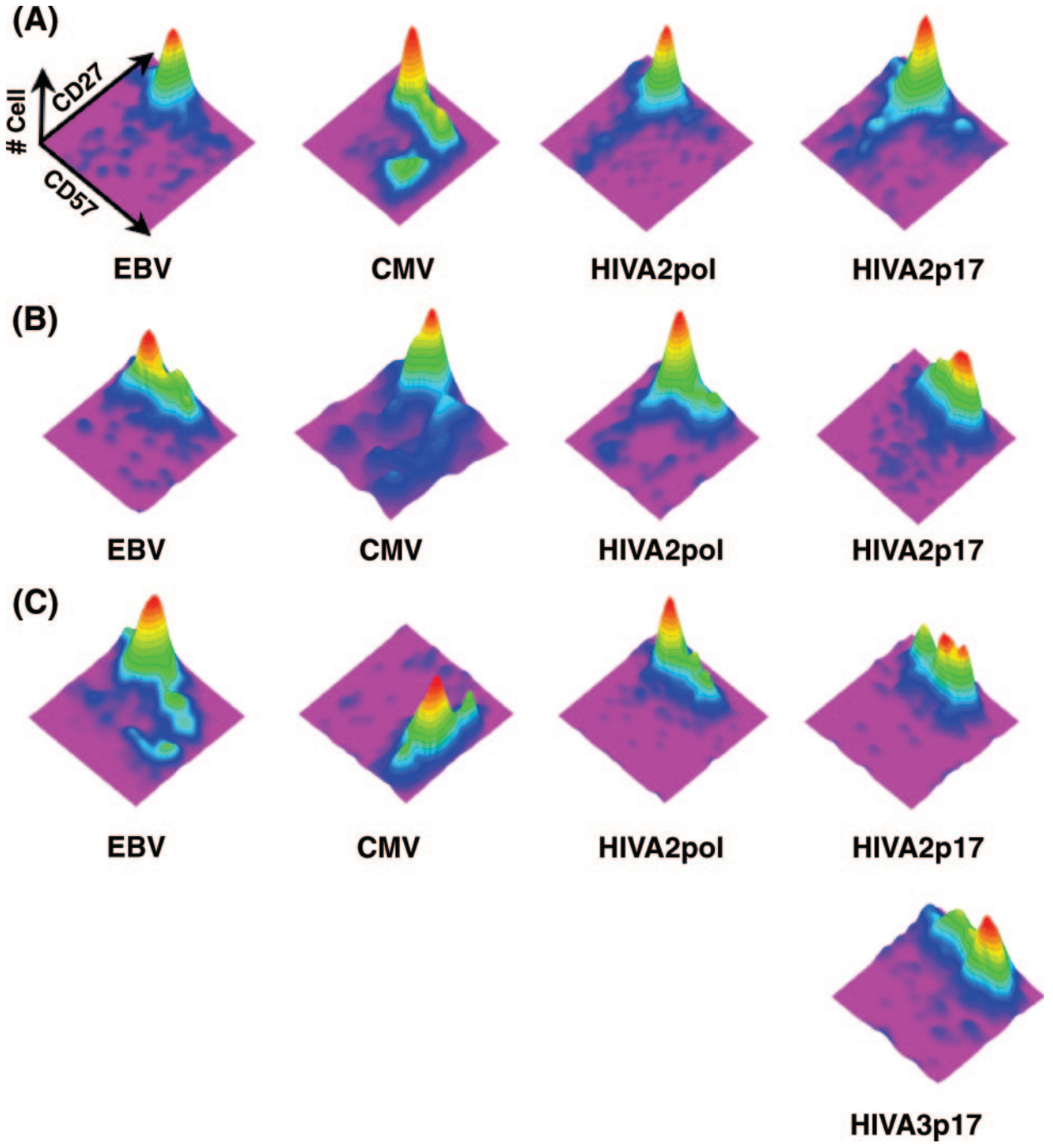

FIG. 3. Pattern of CD27 and CD57 expression on EBV-, CMV-, and HIV-specific $CD8^+$ T cells from three HIV-1-infected participants with a triple tetramer reactivity. Shown are three-dimensional topographical plots of CD27 and CD57 expression on tetrameter-positive $CD8^+$ T cells from participant 3 (A), participant 5 (B), and participant 2 (C). Refer to the legend for Fig. 2F for a description of the topographical plot.

tween disease progression and the development of the $CD27^{high}$ $CD57^{low}$ subset. This question is best addressed by a longitudinal study to determine whether the $CD27^{high}$ $CD57^{low}$ subset arises prior to the loss of immune control of HIV-1 chronic infection. Clearly, further elucidation of the functional significance of the $CD27^{high}$ $CD57^{low}$ subset is warranted.

Our hypothesis as to how the $CD27^{high}$ $CD57^{low}$ subset may develop during chronic HIV-1 infection is that HIV-1-specific $CD8^+$ T cells lose the capacity to undergo differentiation from the early stage ($CD27^{high}$ $CD57^-$) to the effector stage ($CD27^-$ $CD57^{high}$). They instead accumulate as an atypical $CD27^{high}$ $CD57^{low}$ subset, potentially due to the inability for coordinated down-regulation of CD27 and up-regulation of CD57. Recently it has been shown that CD27 down-regulation on CMV-specific $CD8^+$ T cells requires CD70 expression induced by antigen-specific activation and the presence of inter-

leukin-2 (6). Thus, long-term continuous activation of HIV-1-specific $CD8^+$ T cells in the absence of IL-2 due to $CD4^+$ T-cell loss could lead to impaired CD70 expression by activated HIV-1-specific $CD8^+$ T cells.

Alternatively, the effector subset ($CD27^-$ $CD57^{high}$) of HIV-1-specific $CD8^+$ T cells is depleted in tissues and circulation during chronic HIV-1 infection. Interestingly, $CD57^+$ $CD8^+$ T cells are highly susceptible to activation-induced apoptosis (4). Also, chronic antigenic stimulation could deliver an excessive CD27-CD70-mediated costimulatory signal, ultimately leading to the exhaustion of antigen-specific $CD8^+$ T cells (11). Thus, excessive and prolonged CD27-CD70 interaction during chronic HIV-1 infection may cause the deletion of $CD27^-$ $CD57^{high}$ HIV-1-specific $CD8^+$ T cells.

Despite a large number of recent phenotypic and functional T-cell studies, it is still not entirely clear whether a particular phenotypic enrichment or differentiation stage of the virus-specific $CD8^+$ T cells can provide necessary and sufficient protection from chronic viral infection. Intuitively, having a large proportion of the effector subset of virus-specific $CD8^+$ T cells seems to be advantageous because of their capacities to mount immediate protection with direct cytotoxic functions. However, having a large proportion of effector cells may not be suitable for long-term protection if effectors readily undergo activation-induced apoptosis. This issue has remained controversial in the context of assessing phenotypic correlates of long-term survival in HIV-1 infection (3, 13). The mode of long-term nonprogression can be multifaceted, with HIV-1-infected individuals, including long-term survivors, being heterogeneous in their pathogenesis and clinical conditions (e.g., viral load, $CD4^+$ T-cell counts, duration of infection, and types of medications) and bases of immune control of HIV-1 infection.

In conclusion, we assessed the state of differentiation of HIV-1-specific $CD8^+$ T cells by characterizing and comparing phenotypes of HIV-1-, EBV-, and CMV-specific $CD8^+$ T cells based on multiparameter flow cytometry. We found that HIV-1-specific $CD8^+$ T cells predominantly displayed the phenotype $CD27^{high}$ $CD28^-$ $CD57^{low}$ $CD62L^-$. Moreover, our novel finding was that some EBV-specific and a majority of CMV-specific $CD8^+$ T cells displayed coordinated modulation of CD27, CD28, and CD57 expression during T-cell differentiation, while a majority of HIV-1-specific $CD8^+$ T cells did not. Particularly, HIV-1-specific $CD8^+$ T cells did not appear to differentiate to the effector $CD27^-$ $CD57^{high}$ subset but were enriched in the atypical $CD27^{high}$ $CD57^{low}$ subset. There was a marked increase in enrichment of the $CD27^{high}$ $CD57^{low}$subset with chronic disease. Based on these results, we propose a model wherein HIV-1-specific $CD8^+$ T cells sustain impaired effector differentiation during the course of chronic HIV-1 infection.

ACKNOWLEDGMENTS

We are grateful to the Pitt Men's Study participants for their blood donations, Angela M. Alexander and Massimo Trucco for HLA typing, Albert Donnenberg for assistance on data analysis, and Pawel Kalinski and Otto Yang for critical review of the manuscript.

This work was supported by NIH grants R37-AI41870, U01-AI35041, and P01-AI055794 and the AIDS Clinical Trials Group subcontract 204IC006.

REFERENCES

1. **Appay, V., P. R. Dunbar, M. Callan, et al.** 2002. Memory $CD8^+$ T cells vary in differentiation phenotype in different persistent virus infections. Nat. Med. **8:**379–385.
2. **Appay, V., L. Papagno, C. A. Spina, et al.** 2002. Dynamics of T cell responses in HIV infection. J. Immunol. **168:**3660–3666.
3. **Appay, V., and S. L. Rowland-Jones.** 2002. Premature ageing of the immune system: the cause of AIDS? Trends Immunol. **23:**580–585.
4. **Brenchley, J. M., N. J. Karandikar, M. R. Betts, et al.** 2003. Expression of CD57 defines replicative senescence and antigen-induced apoptotic death of $CD8^+$ T cells. Blood **101:**2711–2720.
5. **Chen, G., P. Shankar, C. Lange, et al.** 2001. CD8 T cells specific for human immunodeficiency virus, Epstein-Barr virus, and cytomegalovirus lack molecules for homing to lymphoid sites of infection. Blood **98:**156–164.
6. **Gamadia, L. E., E. M. van Leeuwen, E. B. Remmerswaal, et al.** 2004. The size and phenotype of virus-specific T cell populations is determined by repetitive antigenic stimulation and environmental cytokines. J. Immunol. **172:**6107–6114.
7. **Hoffmann, T. K., V. S. Donnenberg, U. Friebe-Hoffmann, et al.** 2000. Competition of peptide-MHC class I tetrameric complexes with anti-CD3 provides evidence for specificity of peptide binding to the TCR complex. Cytometry **41:**321–328.
8. **Hoji, A., and C. R. Rinaldo.** 2005. Human $CD8^+$ T cells specific for influenza A virus M1 display broad expression of maturation-associated phenotypic markers and chemokine receptors. Immunology **115:**239–245.
9. **Papagno, L., V. Appay, J. Sutton, et al.** 2002. Comparison between HIV- and CMV-specific T cell responses in long-term HIV infected donors. Clin. Exp. Immunol. **130:**509–517.
10. **Papagno, L., C. A. Spina, A. Marchant, et al.** 2004. Immune activation and $CD8^+$ T-cell differentiation towards senescence in HIV-1 infection. PLoS Biol. **2:**E20.
11. **Tesselaar, K., R. Arens, G. M. van Schijndel, et al.** 2003. Lethal T cell immunodeficiency induced by chronic costimulation via CD27-CD70 interactions. Nat. Immunol. **4:**49–54.
12. **van Baarle, D., S. Kostense, E. Hovenkamp, et al.** 2002. Lack of Epstein-Barr virus- and HIV-specific $CD27^-$ $CD8^+$ T cells is associated with progression to viral disease in HIV-infection. AIDS **16:**2001–2011.
13. **van Baarle, D., S. Kostense, M. H. van Oers, D. Hamann, and F. Miedema.** 2002. Failing immune control as a result of impaired $CD8^+$ T-cell maturation: CD27 might provide a clue. Trends Immunol. **23:**586–591.